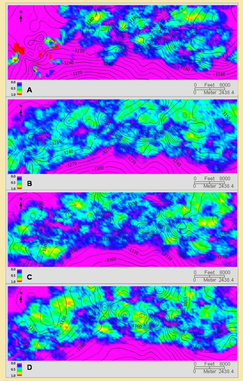

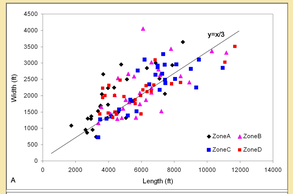

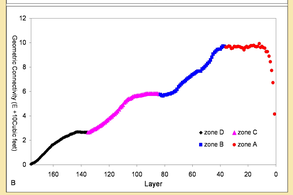

LEFT - Facies proportion maps of oolitic complexes calculated from facies model built using object-based simulation. A) Facies proportion map of oolitic complexes for zone A, overlay of restored structural map of zone A; B) Facies proportion map of oolitic complexes for zone B, overlay of restored structural map of zone B; C) Facies proportion map of oolitic complexes for zone C, overlay of restored structural map of zone C; D) Facies proportion map of oolitic complexes for zone D, overlay of restored structural map of zone D. In all zones, occurrence of oolitic complexes is higher around the edges of the embayment, relative to structurally highest and lowest areas.

RIGHT - A) The distribution of length and width of oolitic deposits, measured from oolitic complexes on top of each St. Louis zone. The ratio of length and width shows a general trend of 3:1. The lateral extent of the oolitic deposits increased from zones D to zone C and B, and then decreased at the top of zone A; B) Geometric connectivity calculated in each modeling layer for oolitic complexes, displaying a general trend of increase from zone D to zones C and B. Within zones D, C, and B, the connectivity curves show a sigmoid shape. The rates of increase in connectivity are slow starting at the bottom, reach a maximum, then decrease toward the top of each zone. The geometric connectivity values are high and relatively stable at the lower part of zone A, and then drop dramatically near the top of zone A.

	Variogram		Azimuth (degree)	Variogram type
	Horizontal range (ft)	Vertical range (ft)		
Oolitic deposit Complex	8345	3370	90	General exponential (power = 0.7)
Cemented oolitic deposit	5237	1890	20	General exponential (power = 0.6)
Eolianite complex	9420	4620	34	95 General exponential (power = 0.7)
Tidal Flat	6080	2990	23	85 General exponential (power = 0.7)
Marine	6670	4580	30	0 General exponential (power = 0.6)

Variogram model of depositional facies in St. Louis Limestone computed from facies curves in the wells and fitted to the variogram model to obtain horizontal and vertical ranges of the facies . Data used to model distribution of facies using indicator simulation with simple kriging and Bayesian kriging.

INDICATOR SIMULATION

Soft Constraint Proportion Map of Oolitic Complexes From Well Data

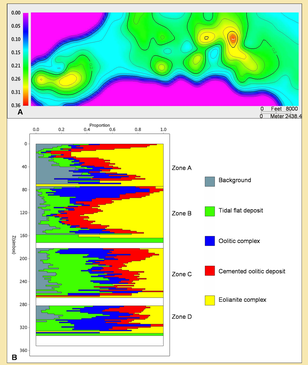

Stochastic Facies Model Indicator Simulation - Simple Kriging

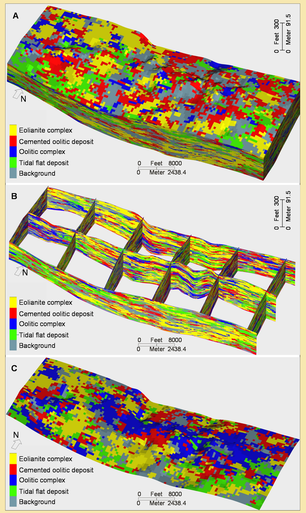

Stochastic Facies Model Indicator Simulation - Bayesian Kriging

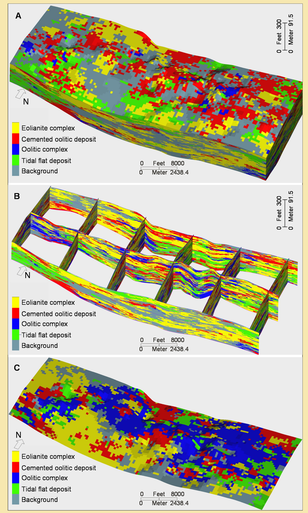

Indicator simulation is a different approach to building facies distributions. Instead of using geometric data to model facies objects, indicator simulation is based on variograms generated from facies curves. The variograms represent both the size and 3D spatial frequency of the facies patterns. Experimental variograms are first computed from facies curves in the wells, and then fitted to the variogram model to obtain horizontal and vertical ranges of the facies. To add geological constraints to the simulation realizations, vertical facies proportion curves and two-dimensional facies proportion maps were built from the well data and used as soft constraint. Two simulations were performed using simple kriging (SK) and Bayesian kriging (BK). The primary axis of the horizontal variogram model was east-west, respecting the general structural orientation. In both simple and Bayesian-derived facies models, oolitic complexes are adjacent to the local highs in the St. Louis Limestone zone B following the trend of the deeper embayment in the south, which is well defined by the facies proportion constraints. The facies model simulated using Bayesian kriging tends to combine nearby similar facies together, and shows more connectivity in the oolitic deposits and more geologically reasonable geometry for facies compared with the facies simulation results from simple kriging. Multiple equally probabilistic realizations are gained by repeating this stochastic procedure.

Compared to the object-based simulation, facies simulated using indicator simulation show a similar overall distribution, but geometric distribution of individual facies is more dispersed and shows decreased lateral and vertical connectivity. Since the facies objects were initially simulated around wells, facies in the object-based model tend to show condensation in the vicinity of the wells even though the same volume proportions were used as in indicator simulations. The dimensions of oolitic complexes (8,845 ft [2654 m] X 3370 ft [1011 m]) and the cemented oolitic deposits (5237 ft [1571 m]X 1890 ft [567 m]) computed by indicator simulation are comparable to the geometry computed with the object-based models.

In both indicator and object-based approaches, the modeled depositional trends, geometry and patterns reflect lithofacies curves and proportion data calculated from well data. The modeled facies distributions support an interpretation of the St. Louis Limestone as a series of oolitic grainstone shoals deposited during fluctuations of relative sea level. Object-based and indicator 3D geostatistical facies models provide similar insights into the uncertainty of facies architecture of the St. Louis Limestone.

Poster available online at: http://www.kgs.ku.edu/PRS/publication/2006/OFR06_04/index.html

SUMMARY AND CONCLUSIONS

Neural network analysis coupled with lithofacies descriptions and available well data provide a basis to construct improved fine-scale facies models using stochastic simulation methods. These models improve our understanding of the distribution and controlling factors on the external geometry of relatively thin ooid grainstone intervals in the St. Louis Limestone of southwest Kansas. Object-based simulation and indictor simulation with kriging were used to build facies distributions of oolitic deposits based on geometric data and lithofacies curves predicted from well logs using a neural network. Within the facies framework, the model illustrates the internal and external geometry and distribution of St. Louis Limestone oolitic reservoirs and associated lithofacies. The fine-scale distribution of rock properties can be assigned to each facies according to the spatial relationship built from variogram analysis. The defined static geological models can be upscaled to run simulations in order to explore responses to fluid flow.

The following specific conclusions are drawn from this study:

1. Three-dimensional spatial distributions of the St. Louis Limestone oolitic reservoirs are modeled and explored with object-based simulation and indicator simulation with kriging. Results illustrate that the location of structural highs and general trends at the time of deposition had an impact on distribution and orientation of the St. Louis Limestone oolitic complexes. Oolitic deposits formed linear belts along the edge of a local embayment trending approximately northwest-southeast, while additional shoals were formed on the platform adjacent to, but not on, local highs.

2. The observed pattern change in the lateral extent and geometric connectivity of modeled oolitic deposits from zone D to zone A suggests the overall agradation of oolitic deposits during relative rise in sea level (zone D to zone B) followed by deepening near the top of the St. Louis Limestone prior to erosion at the base of the Ste. Genevieve Limestone.

3. Oolitic deposits are generally absent in the center of the embayment. Modeled oolitic complexes illustrate an agradational and the slightly progradational depositional pattern as they accumulated from zone D through zone A. Eolianite deposits show a back-stepping depositional pattern and some were accumulated on the local structural highs and some in the local lows on the slope. Eolianite deposits abundance and thickness increase upward from zone D to zone A. Tidal flat deposits are thinner, laterally extensive, and accumulate and thicken into the structural lows and toward the embayment. The content of tidal-flat deposits decreases from the bottom to the top within each zone, and is interpreted as indicating transgression and followed by agradation of shallow-marine to non-marine facies within each zone.

4. Eolianite complexes are better represented at locations where oolitic complexes are relatively thin (i.e., structural highs and localized low areas on the slope). The processes that deposited the oolitic complexes eroded the previously deposited eolianite complexes and tidal-flat deposits.

5. The cemented oolitic deposits have been modeled as barrier/baffle layers among the oolitic complexes and are concentrated at their edges.

6. Uncertainty and variability of the external and internal geometry of the St. Louis Limestone oolitic reservoirs were explored using stochastic simulation methods, producing multiple equally probabilistic realizations.

7. Object-based simulation produced more geologically reasonable facies distributions than indicator simulation. The different geostatistical approaches produce similar facies patterns and provide support to the interpretation. Because of relatively high well density, object-based simulation required longer computation times than indicator simulation.

8. The results and statistical models are useful for understanding the geometry of oolitic complexes or other shallow marine sand bodies. The methodology can be implemented in complex depositional systems without seismic data.

ACKNOWLEDGEMENTS

The Kansas Geological Survey provided financial support as part of Lianshuang Qi's dissertation research. Thanks to Geoff Bohling and Marty Dubois for discussions, assistance, and comments. Special thanks to Dana Adkins-Heljeson for his assistance and comments on the open-file reports. We would like to thank Roxar Corporation for providing access to Reservoir Modeling System (RMS) and Geoplus Corporation for access to PETRA.